Tikhonov regularization aided quantitative susceptibility mapping of whole brain without background field removal

Hongfu Sun, M. Ethan MacDonald, Yuhan Ma, G. Bruce Pike
Department of Radiology, Cumming School of Medicine, University of Calgary, Canada

UNIVERSITY OF CALGARY

BACKGROUND

- A background field removal step is usually required before the actual inversion. However, it is problematic near the edge of the brain.
- Single-step QSM methods have been proposed by combining the background field removal with inversion (1,2). However, it still erodes the brain edge.
- A recent study proposed a total field inversion method using R2* map as a preconditioner to boost the convergence speed (3).
- Here we propose an inversion method that also performs direct deconvolution on the total field map by adding a Tikhonov regularization to aid the more ill-posed inversion, in addition to the traditional TV regularization.

METHODS

- **Tikhonov regularization aided QSM (Tik-QSM)**

The induced magnetic field perturbation ΔB is the convolution of the magnetic dipole field kernel D with the susceptibility source χ:

$$\boldsymbol{F^{-1}DF\chi = \Delta B/B_0 = \delta B}$$

However, induced field can only be measured in the brain tissue region $M\delta B$. So the least-squared minimization is formulated as:

$$\boldsymbol{argmin_\chi \left\| MF^{-1}DF\chi - M\delta B \right\|_2^2}$$

This inversion becomes more ill-posed due to additional zeros in the brain mask M term. To assist the inversion, a Tikhonov regularization of the local tissue susceptibility $M\chi$ is applied in addition to the traditional TV regularization:

$$\boldsymbol{argmin_\chi \left\| MF^{-1}DF\chi - M\delta B \right\|_2^2 + \lambda_1 \|M\chi\|_2^2 + \lambda_2 TV(M\chi)}$$

where λ_1 and λ_2 are regularization parameters for Tikhonov and TV regularization respectively. The theory behind is that the background susceptibility $(1 - M)\chi$ is about two orders of magnitude greater than local susceptibility $M\chi$, and therefore background susceptibility is responsible for the majority of the measured total field inside the brain tissue region and is given complete freedom for dipole fitting, on the contrary, local tissue susceptibility is assumed to be relatively small and is therefore constrained with the Tikhonov regularization.

- **Image reconstruction**

The QSM reconstruction pipeline is illustrated in Fig. 1 starting from raw phase images from 8 bipolar echoes. An initial receiver-coil phase-offset correction was applied to the raw phase. Briefly, the correction method calculates the underlying phase-offsets from odd and even echoes respectively using a dual-echo approach, and removes them from the raw phase in the complex manner without phase unwrapping process (4).

Tik-QSM was solved using the non-linear conjugate gradient method. To compare with traditional two-step QSM methods, the total field was also processed by RESHARP and PDF methods for background field removal. TV regularized susceptibility inversion was then performed on both local field maps. A spherical kernel of 5 voxels was used for RESHARP resulting in RESHARP-QSM of 5 voxels edge erosion, while full brain was kept for PDF-QSM.

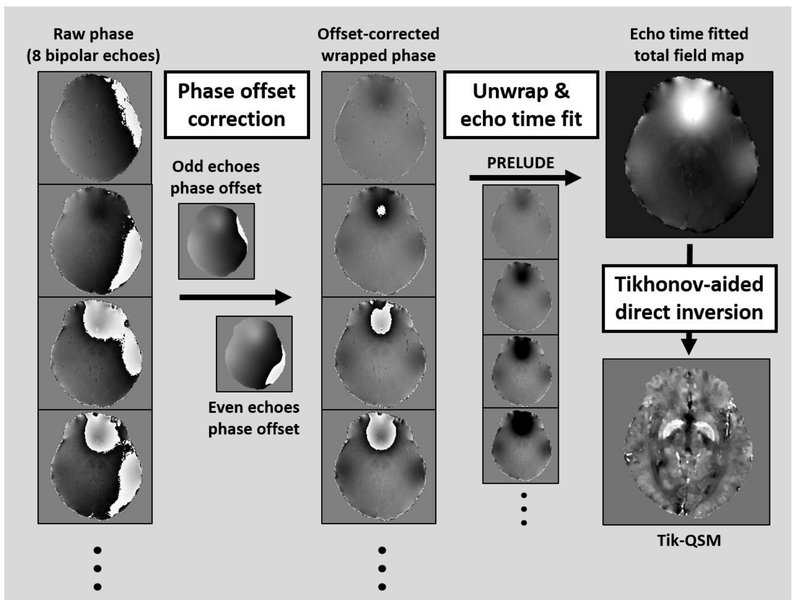

Fig. 1: Tik-QSM reconstruction pipeline.

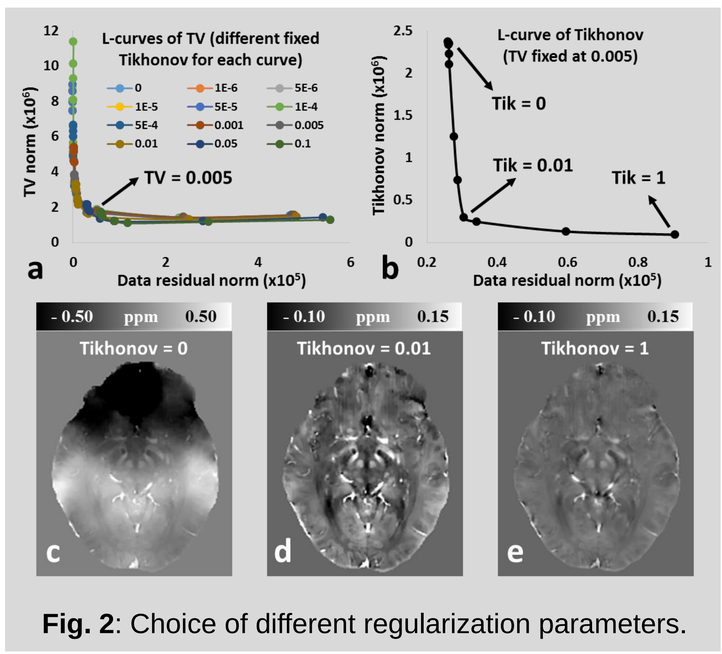

Fig. 2: Choice of different regularization parameters.

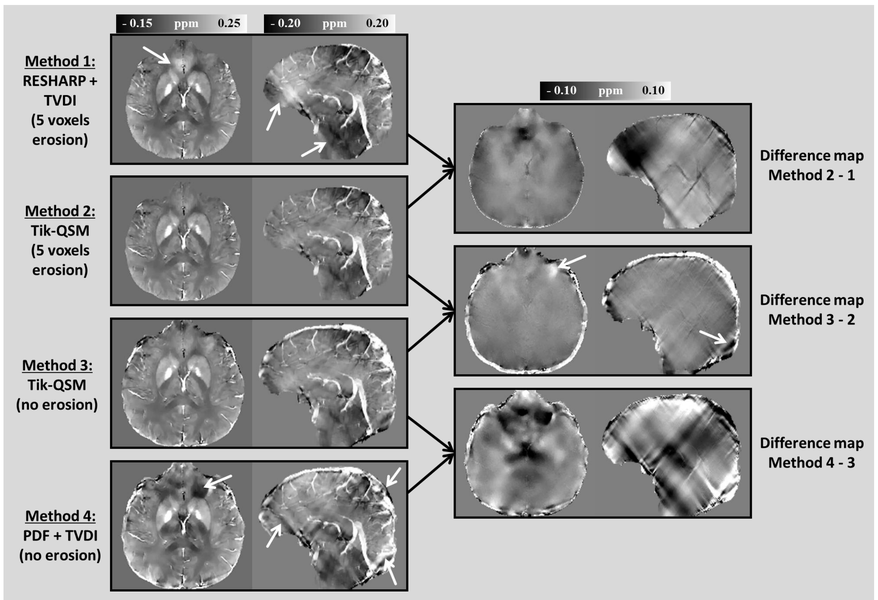

Fig. 3: comparison of different QSM reconstruction methods.

RESULTS

- **Regularization parameters and L-curves**

A parametric sweep of λ_1 and λ_2 was performed on one subject, with both values ranging from [0, 10^{-6}, $5*10^{-6}$, 10^{-5}, $5*10^{-5}$, … 1]. For each fixed λ_2, an L-curve of the TV norm was formed with all λ_1 values as shown in Fig. 2a. All L-curves, with different λ_1, have the maximum curvature around $\lambda_2 = 0.005$, which represents the optimal TV regularization parameter. Once λ_2 is fixed at 0.005, an L-curve of the Tikhonov regularization was plotted in Fig. 2b. The maximum curvature occurs around $\lambda_1 = 0.01$.

To demonstrate the effect of different Tikhonov regularization parameters, the Tik-QSM results of full brain with λ_1 of 0 (equivalent to TV regularization only), 0.01 and 1 were shown in Fig. 2c-e, representing the cases of under-, optimal- (corner of L-curve) and over-regularizations. Large artefact presents in (c), while susceptibility contrast is substantially suppressed in (e). These two factors are well balanced in (d).

- **Comparison of Tik-QSM with two-step QSM**

QSM results from 4 different reconstruction methods were shown in Fig. 3. Part of the superior sagittal sinus was eroded in RESHARP and the mask-matched Tik-QSM (Method 2), while kept in full-brain Tik-QSM and PDF. Difference maps of the methods were calculated by subtracting the top images from the bottom images and were shown on the right in Fig. 3.

Tik-QSM methods show suppressed artefacts compared with RESHARP or PDF methods. Large brain mask tends to introduce more artefacts than the eroded version near the edge of their common area. However, the image qualities of the inner brain remain similar between the two masks. PDF does not erode the brain mask and gives QSM of full brain. However, susceptibilities at the brain edge using PDF are not accurate and are usually contaminated with noticeable artefacts as evident in the difference map of PDF vs. Tik-QSM of full brain.

DISCUSSION AND CONCLUSION

- The proposed Tik-QSM method eliminates the need for a separate background field removal step before inversion.
- A Tikhonov regularization term constraining the local susceptibility distribution is added to assist the inversion.
- The optimal regularization parameters were chosen based on the L-curve method, balancing between artefacts and contrast.
- The Tik-QSM method shows artefact reduction over the traditional two-step methods (RESHARP and PDF).
- This method can keep the whole brain volume, which enables QSM in cortical grey matter such as functional QSM (5) and whole brain QSM venography (6).

REFERENCES

(1) Liu T, Wang Y, et al. ISMRM 2014, Milan , p597.
(2) Langkammer C, Ropele S, et al. NeuroImage 2015: 622-630.
(3) Liu Z, Spincemaille P, et al. MRM 2016.
(4) Sun H, Pike GB, et al. ISMRM 2016, Singapore, p2987.
(5) Balla D, Bowtell R, et al. NeuroImage 2014: 112-124.
(6) Fan A, Adalsteinsson E, et al. MRM 2014:149-159.

Alberta Innovates Health Solutions